

Current-voltage characteristic of a double tunnel junction under Coulomb-blockade conditions

V. Shikin, S. Leao,¹⁾ and O. Hipólito¹⁾

Institute of Solid State Physics, Russian Academy of Sciences

(Submitted 22 September 1992)

Zh. Eksp. Teor. Fiz. **103**, 655–665 (February 1993)

The question of the correspondence between the current-voltage characteristic and the stability diagram for a double tunnel junction under Coulomb-blockade conditions is taken up. It is shown that there is indeed such a correspondence. The role played by the temperature in shaping the peaks in the conductance of the junction is studied. Possibilities for using the results of this study for the diagnostics of double tunnel junctions are discussed.

Various effects of Coulomb origin in tunnel junctions with small dimensions were first observed many years ago in granular materials.^{1–4} Recent technological process has made it possible to reproduce these effects (“Coulomb-blockade effects”) at individual tunnel junctions with adjustable parameters.⁵ The experimental opportunities in this field have expanded substantially as a result. In particular, the system consisting of a double tunnel junction with a Coulomb barrier of adjustable height has won widespread popularity.⁶ Figure 1 shows an example of this system. The tunneling current I through the system of two tunnel junctions C_i and C_j arises at a transport voltage $V \neq 0$. In addition, a control voltage V_g which affects I is applied through the capacitance C_g to the gap (“island”) between capacitors C_i and C_j . The tunneling current is suppressed as a result of the discrete nature of the charge of an electron under the conditions

$$\frac{e^2}{2C} > T, \quad \frac{e^2}{2C} < eV, \quad C = C_i + C_j + C_g. \quad (1)$$

If V_g is varied monotonically, oscillations arise in this current^{3,6} with a period ΔV_g :

$$C_g \Delta V_g = |e|. \quad (2)$$

In general, the current I at a fixed temperature T is thus a nonlinear function of V and V_g . We will call this functional dependence the “conditional current-voltage characteristic” or “ I - V - V_g characteristic.”

One specific problem which has yet to be clearly resolved is whether there is a correspondence between the current-voltage characteristic and the stability diagram for a controlled double tunnel junction in the limit $T \rightarrow 0$. The “stability diagram” is a periodic system of rhombi in the V , V_g plane [with a period ΔV_g ; see (2)]. Within each of these rhombi, whose corners are at positions which depend on the quantities C_i , C_j , C_g , the tunneling current I is zero in the limit $T \rightarrow 0$. The properties of this diagram are discussed in Ref. 5, among other places (see Fig. 4 of that paper and the associated discussion). The boundaries of these rhombi are given by relations (12) and (13) below. An important point is that these boundaries depend only on the equilibrium characteristics of the double tunnel junction. On the other hand, the current-voltage characteristic is a kinetic characteristic of a junction. Appearing in the definition of this characteristic, along with the equilibrium parameters, are the transmission levels λ_i and λ_j of the barriers C_i and C_j . Con-

sequently, it is not self-evident that the conductance peaks would lie precisely in the “windows” of the stability diagram. The existence of a correspondence of this sort between the stability diagram and the current-voltage characteristic for a double tunnel junction in the limit $V \rightarrow 0$ has been pointed out by Glazman and Shekhter.⁷ In the present paper, those results are generalized to nonzero values $V \neq 0$.

The information derived below is useful for the diagnostics of double tunnel junctions. The existing methods for determining the capacitances C_i and C_j from the activation-law temperature dependence of the conductance of the double junction near its minima and from the threshold for the appearance of a current in the region $e^2/c > eV$ suffer from disadvantages which reduce the accuracy with which C_i and C_j are determined. In the first case, the minimum conductance usually ceases to be a “one-particle” conductance, since two-particle tunneling events contribute significantly near the minima.⁸ With regard to threshold-based estimates of C_i and C_j , we note that the heating of the electron system apparently becomes important in this case. In this sense, a reconstruction of the stability diagram from the known properties of the I - V - V_g characteristic may prove useful for finding an independent estimate of the parameters of the problem. This capability is important for testing the predictions of the existing theory for the Coulomb blockade in double tunnel junctions.

1. For the system shown in Fig. 1, the Coulomb eigenstates E_{nm} which are part of the Coulomb-blockade theory are⁵

$$\begin{aligned} CE_{nm} &= \frac{1}{2} [(n+m)e - C_g V_g]^2 + enV(C_i + \frac{1}{2} C_g) \\ &\quad - emV(C_j + \frac{1}{2} C_g), \\ C &= C_i + C_j + C_g, \quad n, m = 0 \pm 1 \pm 2 \dots \end{aligned} \quad (3)$$

Here m corresponds to an electron jump to the island through the capacitance C_i , while n has the corresponding meaning for a jump through the capacitance C_j .

The differences

$$E_{nm} - E_{n-1, m} = \varepsilon_l - \varepsilon_{l-1} - eV_1, \quad (4)$$

$$E_{nm} - E_{n, m-1} = \varepsilon_l - \varepsilon_{l-1} - eV_2, \quad (5)$$

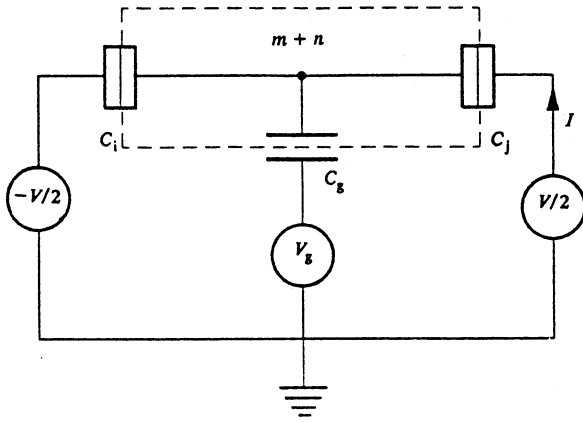


FIG. 1. Circuit diagram of a double tunnel junction.

$$\varepsilon_l = \frac{1}{2C} (eV - C_g V_g)^2, \quad l = n + m, \quad (6)$$

$$eV_1 = eV \frac{C_l + C_g/2}{C}, \quad eV_2 = -eV \frac{C_j + C_g/2}{C} \quad (7)$$

have a structure similar to that of corresponding combinations in Coulomb-blockade theory for double tunnel junctions.⁴ We can therefore use the formalism of Ref. 4 to determine the I - V - V_g characteristic for the system in Fig. 1. According to the present understanding of the properties of double tunnel junctions under Coulomb-blockade conditions,⁹ the formalism of Ref. 4 is meaningful under the condition

$$Z(\omega) < h/e^2,$$

where $Z(\omega)$ is the impedance of the external circuit. This is a reasonable approximation for double tunnel junctions.

We accordingly use the results of Ref. 4 to write an expression for the steady-state current I through the double tunnel junction in Fig. 1:

$$I(T, V, V_g) = e \lambda_i \sum_l \{W_{l-1} f(-\Delta\varepsilon_l + eV_2) - W_l f(\Delta\varepsilon_l - eV_2)\}, \quad (8)$$

$$\Delta\varepsilon_l = \varepsilon_l - \varepsilon_{l-1}, \quad (8a)$$

$$f(x) = \frac{x}{1 - \exp(-\beta x)}, \quad \beta = T^{-1}, \quad (9)$$

$$\lambda_i = 4\pi T_i^2 N_i(0) N_f(0), \quad \lambda_j = 4\pi T_j^2 N_j(0) N_f(0).$$

Here ε_l are the energies from (6); $N_i(0)$, $N_j(0)$, and $N_f(0)$ are the densities of states at the Fermi surface for the electrode to the left of contact C_l , for the electrode to the right of C_j , and for the island; and T_i and T_j are the corresponding tunneling matrix elements.

To find the probabilities W_l we must solve the kinetic equation for W_l . This equation was derived from first principles in Ref. 4. Under the conditions $W_l = 0$, it leads to the algorithm

$$W_{l-1} = W_l \frac{\lambda_j f(\Delta\varepsilon_l - eV_1) + \lambda_i f(\Delta\varepsilon_l - eV_2)}{\lambda_j f(-\Delta\varepsilon_l + eV_1) + \lambda_i f(-\Delta\varepsilon_l + eV_2)}, \quad (10)$$

which relates W_{l-1} to W_l .

Using (10), we find from (8)

$$I = e \lambda_i \sum_l W_l \left\{ \frac{\lambda_j f(\Delta\varepsilon_l - eV_1) + \lambda_i f(\Delta\varepsilon_l - eV_2)}{\lambda_j f(-\Delta\varepsilon_l + eV_1) + \lambda_i f(-\Delta\varepsilon_l + eV_2)} \times f(-\Delta\varepsilon_l + eV_2) - f(\Delta\varepsilon_l - eV_2) \right\}. \quad (11)$$

Using this expression, we can identify some general properties of the current I , which are independent of the particular form of W_l . In particular, the expression for I in (11) is sufficient for solving questions regarding the correspondence between the current-voltage characteristic and the stability diagram.

The formal boundaries on the stability diagram arise from an analysis of the explicit expression (3) for the energies E_{nm} . They ultimately reduce to a description of two families of straight lines in the V , V_g plane:

$$\Delta\varepsilon_l - eV_1 = 0, \quad (12)$$

$$\Delta\varepsilon_l - eV_2 = 0, \quad (13)$$

where V_1 and V_2 are from (7), and $\Delta\varepsilon_l$ is from (8a). On these lines, in the limit $T \rightarrow 0$, the current I in (11) should vanish:

$$I(T, V, V_g, \lambda_i, \lambda_j) \Big|_{\substack{T \rightarrow 0 \\ \Delta\varepsilon_l - eV_1 \rightarrow 0 \\ \Delta\varepsilon_l - eV_2 \rightarrow 0}} \longrightarrow 0 \quad (14)$$

Some asymptotic properties of the function $f(x)$ in (9) are important for proving (14):

$$f(x) \Big|_{\substack{x \rightarrow 0 \\ \beta \rightarrow \infty}} = f(-x) \Big|_{\substack{x \rightarrow 0 \\ \beta \rightarrow \infty}} = 0. \quad (15)$$

Also of importance is the property

$$f(x)/f(-x) = \exp(\beta x). \quad (16)$$

With (15) in mind, we examine the behavior of I in (11) under the condition (12):

$$I \Big|_{T \rightarrow 0} \propto \sum_l W_l \left\{ \frac{\lambda_j f(0) + \lambda_i f(\Delta\varepsilon_l - eV_2)}{\lambda_j f(0) + \lambda_i f(-\Delta\varepsilon_l + eV_2)} f(-\Delta\varepsilon_l + eV_2) - f(\Delta\varepsilon_l - eV_2) \right\} = \sum_l W_l \{f(\Delta\varepsilon_l - eV_2) - f(\Delta\varepsilon_l - eV_2)\} = 0. \quad (11a)$$

In other words, the necessary property (14) is exhibited here.

Using (15) and (16), we find the following result on the boundaries (13):

$$I \propto \sum_l W_l \left\{ \frac{f(\Delta\varepsilon_l - eV_1)}{f(-\Delta\varepsilon_l + eV_1)} f(0) - f(0) \right\}$$

$$= \sum_l W_l \{ \exp(-\beta|eV|) f(0) - f(0) \} = 0. \quad (11b)$$

The current I in (11) thus vanishes at the boundaries (13).

Assertions (11a) and (11b) answer in the affirmative the question of whether there is a correspondence between the current-voltage characteristic and the stability diagram; formally, the matter reduces to conditions (14).

2. For assistance in the use of the result derived above for diagnostics of double tunnel junctions under Coulomb-

blockade conditions, we will also examine the role played by the temperature in shaping the conductance peaks. For this purpose we use the expression for the current $I(T, V, V_g)$ in the limiting case of a very asymmetric double junction, with, for example,

$$\lambda_i/\lambda_j \gg 1. \quad (17)$$

In this version of the problem, according to Ref. 4, the probabilities W_l cease to depend on λ_i and λ_j and can be found explicitly:

$$W_l = z^{-1} \exp(-E_l/T), \quad \sum_l W_l = 1,$$

$$2CE_l \equiv 2CE_{om} = [eI - (C_g V_g - C_j V - \frac{1}{2} C_g V)]^2, \quad (18)$$

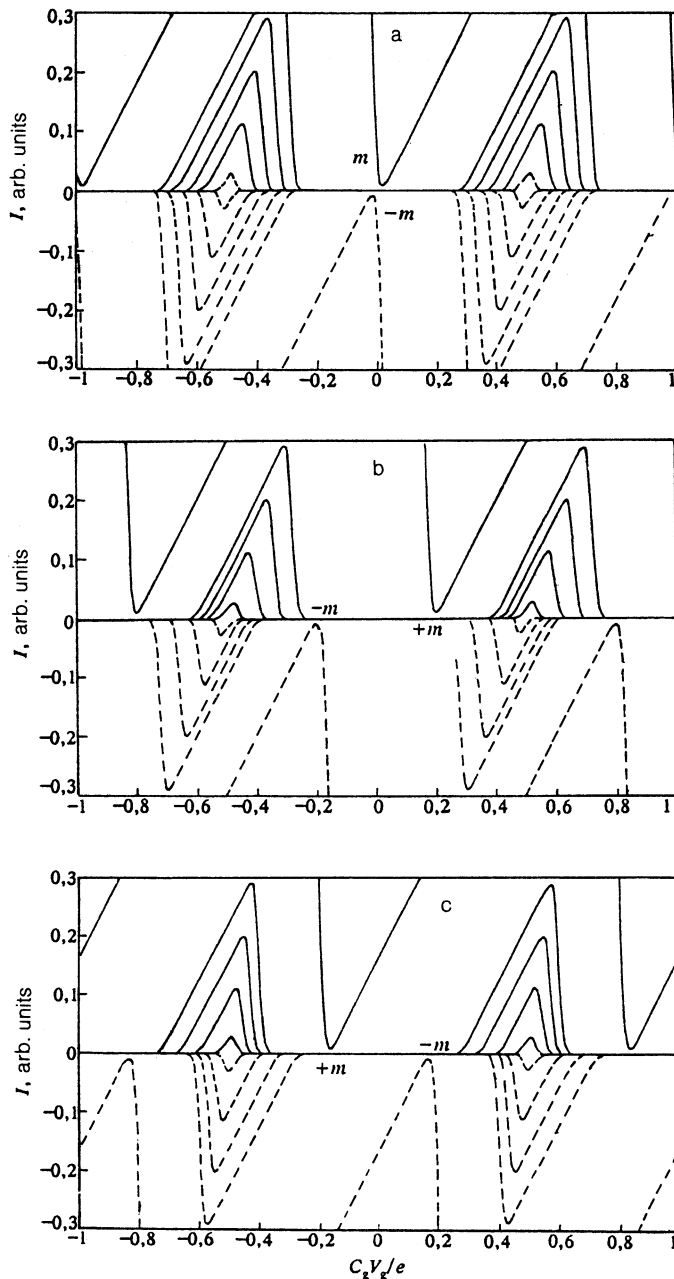


FIG. 2. Current-voltage characteristic corresponding to (19) with the parameter values $T = 20$ mK; $V = \pm 12.5, \pm 37.5, \pm 62.5, \pm 87.5, \pm 260 \mu\text{V}$, $\Delta = 3.0$; and various values of ε . a— $\varepsilon = 0$; b— $\varepsilon = +1.3$; c— $\varepsilon = -1.3$. The points $\pm m$ are positions of the threshold extrema in the conductance (at larger values of V , the double tunnel junction is fully conducting).

We then find

$$I \propto \frac{\text{sh}(eV/2T)}{\delta e^{\delta/4}} \sum_l \frac{\delta(l + \xi' - 1/2)}{\text{sh} \delta(l + \xi' - 1/2)} \frac{\exp\{-\delta(l + \xi'' - 1/2)^2\}}{\sum_n \exp\{-\delta(n + \xi'')^2\}},$$

$$\delta = e^2/2CT, \quad \xi' = \frac{1}{e} [C_g V_g + (C_i + \frac{1}{2} C_g) V], \quad (19)$$

$$\xi'' = \frac{1}{e} [C_g V_g - (C_j + \frac{1}{2} C_g) V].$$

Figure 2, a-c, shows the behavior of the current-voltage characteristic (19) as a function of the combination $C_g V_g/e$ for various values of V at $T = 20$ mK for the parameter values

$$C_g = 73 \cdot 10^{-18} \Phi, \quad \frac{C_i}{C_g} = \Delta - \varepsilon, \quad \frac{C_j}{C_g} = \Delta + \varepsilon \quad (20)$$

with $\Delta \approx 3.0$ and $\varepsilon \approx 1.3$. We will discuss this choice of parameter values a bit further on.

The combination eV/T in these figures varies over the interval

$$7 \leq \frac{eV}{T} \leq 50. \quad (20a)$$

In this interval of eV/T values, the temperature plays only a minor role in shaping the conductance peaks, and the boundaries of the peaks shift linearly with V [in accordance with the predictions (12) and (13)]. In particular, the relative positions of the points $\pm m$, corresponding to the maximum values of V , at which the current is zero at one point at least (for a given cycle) on the $C_g V_g/e$ axis, are given by

$$(+m) - (-m) = \frac{C_j - C_i}{C} = \frac{2\varepsilon}{2\Delta + 1}. \quad (21)$$

This equation follows from the stability diagram.

It should also be noted that in limiting case (17) the position of the conductance peak is a linear function of V , and the shift of this peak along the $C_g V_g/e$ axis as a function of V is independent of the transmission levels λ_i and λ_j :

$$\frac{\delta V_g}{\delta V} = \Delta + \varepsilon + \frac{1}{2}. \quad (22)$$

The relationship (22) can be tested (for example) numerically with the help of (19). We chose the values for the parameters Δ and ε in (20) on the basis of relations (21) and (22) and corresponding experimental data from Ref. 10 (see Fig. 5 in Ref. 10).

It is convenient to conduct this discussion of the effect of the temperature in terms of an effective width $L(T, V)$ of the conductance peak:

$$L(T, V) = \frac{\int_{-\infty}^{+\infty} I(T, V, V_g) d(C_g V_g/e - 1/2)}{I_{\max}(T, V, V_g)}. \quad (23)$$

This quantity is shown in Fig. 3 as a function of the parameter eV/T for the current-voltage characteristic (19). In the region $eV/T \gg 1$, the quantity L is evidently linear in V . In the region $eV/T < 1$, in contrast, there is a saturation in the behavior of $L(T, V)$. However, the asymptotic quantity $L_\infty(V)$, which corresponds to the behavior of $L(T, V)$ at $eV/T \gg 1$, should cross zero when a continuation is made to the region $eV/T < 1$, as can be seen in Fig. 3.

The functional dependence $L(T, 0) \equiv L_0(T)$ is useful in its own right. According to (19), the position of the $L_0(T)$ plateau is a linear function of the temperature and can be described by

$$L_0(T) = \alpha \frac{T}{V_c}, \quad V_c = \frac{e^2}{C}, \quad \alpha \approx 5. \quad (24)$$

The value of α is found numerically (Fig. 4).

In the region $eV/T < 1$ the width of the conductance peaks should thus be a linear function of the temperature [for one-particle approximation (19)]. The slope of this plot gives us direct information on the total capacitance C of the double tunnel junction.

3. The literature reveals no special test of the validity of the necessary conditions (12), (13), and (24) in research on the current-voltage characteristics of double tunnel junctions under Coulomb-blockade conditions. Therefore, all we

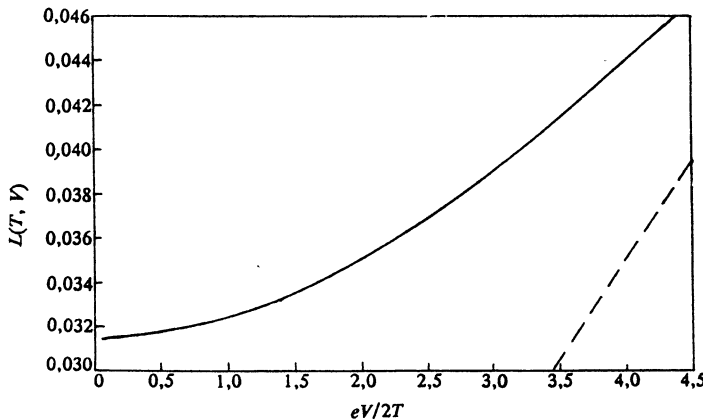


FIG. 3. Plot $L(T, V)$ versus the parameter $eV/2T$. The dashed line shows the asymptotic behavior $L_\infty(V)$; it passes through the point $V = 0$ at $eV/2T \ll 1$.

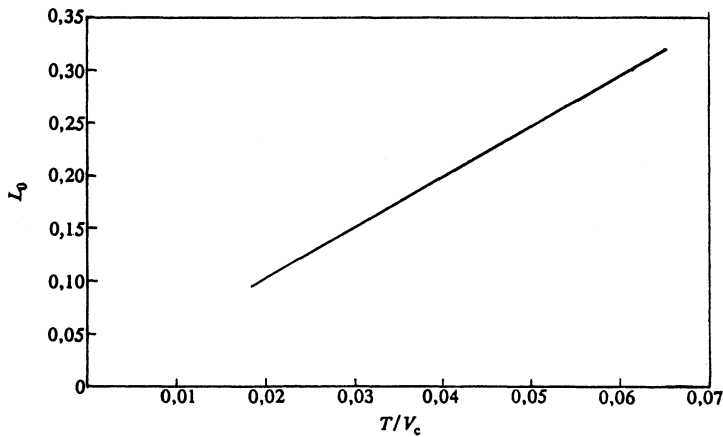


FIG. 4. Behavior of L_0 as a function of T/V_c , where $V_c = e^2/c$, according to expression (19) for $I(T, V, V_g)$ in the limit $eV/T \ll 1$. The number α is a measure of the slope of $L_0(T)$.

can do here is comment on a few pieces of published data which bear on our problem.

In only one paper¹⁰ of which we are aware is the behavior of the tunneling current I as a function of V and V_g described fairly comprehensively. The overall picture of $I(T, V, V_g)$ in these experiments corresponds to the structure of the conductance peaks in Fig. 2b. Making the additional assumption that the double tunnel junction is highly asymmetric, we can thus choose the values of the coefficients Δ and ε from (20) with the help of (21) and (22). The behavior of the boundaries of the conductance peaks found experimentally in Ref. 10 is shown in Fig. 5. We see some deviations which are inexplicable in terms of a one-particle theory of the Coulomb blockade. The problem is that the linear plots in Fig. 5 should converge at the point $V = 0$ (according to the discussion of Fig. 3). The experimental boundaries of the conductance peaks from Ref. 10 obviously do not exhibit this behavior, so it is difficult to pursue the interpretation of the data of Ref. 10 on the basis of a one-particle theory.

A linear temperature dependence of the width of the conductance peaks was observed under the condition $eV/T < 1$ in Ref. 11 (see Fig. 14 of that paper). However, the direct use of the results of the present paper to analyze the data of Ref. 11 is not really legitimate, since in this case the

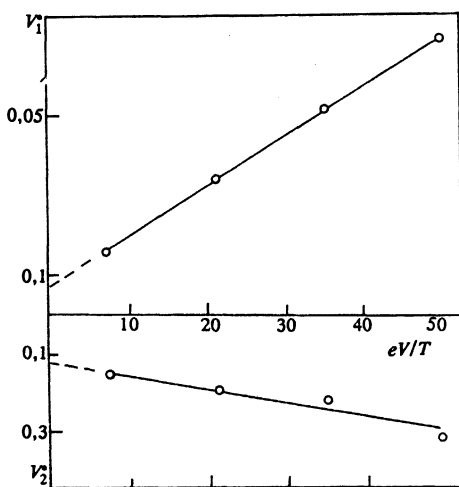


FIG. 5. Experimental data of Ref. 10 on the combinations $V_1^* = V_1/\Delta V_g$ and $V_2^* = V_2/\Delta V_g$, where $V_1(V)$ and $V_2(V)$ are from (7), and ΔV_g is from (2). In this case the asymptotic plots $V_1^*(V)$ and $V_2^*(V)$ do not pass through the point $V = 0$. The temperature corresponding to the experiments of Ref. 10 is $T = 20$ mK.

dimensions of the island are fairly small, and the quantum size effect in the energy of the electrons in the island must be taken into account.

Finally, we turn to the interesting study by Glattli *et al.*⁸ They presented some persuasive arguments in favor of a correlated passage of electrons through a double barrier under conditions such that the conductance of the system is a minimum. However, a quantitative analysis of the results of Ref. 8 with the help of the results of Refs. 12 and 13, in which the perturbation theory of Ref. 4 was extended to the case of multiparticle effects, is problematical. The difficulty is that in the region of maximum conductance in the experiments of Ref. 8—in the region in which the one-particle perturbation theory should work well—the width of the conductance peaks was essentially independent of the temperature, in contradiction of condition (24) (in Fig. 3 of Ref. 8, the peaks at 300 and 35 mK have approximately the same width). Before we attempt a quantitative interpretation of subtle multiparticle tunnel effects, we thus need a more careful study of the region of one-particle effects in this system.

CONCLUSION

We have studied the question of the correspondence between the current-voltage characteristic and the stability diagram for a double tunnel junction under Coulomb-blockade conditions. This necessary condition, formulated as assertion (14), does indeed hold, as is demonstrated by Eqs. (11a) and (11b). These results make it possible to use (12) and (13) to reconstruct the stability diagram of this system from data on the current I as a function of V and V_g .

We have discussed some qualitative aspects of the effect of a nonzero temperature on the shape of the conductance peaks. The linear $L_0(T)$ dependence in (24) and also the possibility of extracting data on the total capacitance C from this dependence are of interest for diagnostics of double tunnel junctions.

Yet another interesting aspect of the situation is the behavior of the position of the conductance peaks. We have studied this aspect only in the limiting case in which the double junction is highly asymmetric [condition (17)]. In this limit, the shift of the conduction peak is described by (22), and it, too, is useful for diagnostics. In the general case $\lambda_i \neq \lambda_j$, however, the position of the peak apparently becomes sensitive to λ_i and λ_j , so the study of this interesting and well-defined aspect of the current-voltage characteristic should be pursued.

The results derived here are pertinent to existing experimental data and will be of assistance in drawing concrete conclusions regarding the validity of one-particle Coulomb-blockade theory for interpreting these experiments.

¹São Carlos Institute of Physics and Chemistry, São Paulo University, Brazil.

¹C. A. Neugebauer and M. B. Webb, *J. Appl. Phys.* **33**, 74 (1962).

²I. Giaever and H. R. Zeller, *Phys. Lett.* **20**, 1504 (1968).

³J. Lambe and R. C. Jaklevic, *Phys. Rev. Lett.* **22**, 1371 (1969).

⁴I. O. Kulik and R. I. Shekhter, *Zh. Eksp. Teor. Fiz.* **68**, 623 (1975) [*Sov. Phys. JETP* **41**, 308 (1975)].

⁵H. Grabert, *Z. Phys. B* **85**, 319 (1991).

⁶T. A. Fulton and G. J. Dolan, *Phys. Rev. Lett.* **59**, 109 (1987).

⁷L. Glazman and R. Shekhter, *J. Phys. Cond. Matt.* **1**, 5811 (1989).

⁸D. Glatli, C. Pasquier, U. Meirav, F. Williams, Y. Jin, and B. Etienne, *Z. Phys. B* **85**, 375 (1991).

⁹H. Grabert, G. Ingold, M. Devoret, D. Esteve, H. Pothier, and G. Urbina, *Z. Phys. B* **34**, 143 (1991).

¹⁰P. Lafarge, H. Pothier, E. R. Williams, D. Esteve, C. Urbina, and M. Devoret, *Z. Phys. B* **85**, 327 (1991).

¹¹U. Meirav, P. McEuen, M. Kastner, E. Foxman, A. Kumar, and S. Wind, *Z. Phys. B* **85**, 357 (1991).

¹²D. Averin and A. Odintsov, *Phys. Lett. A* **140**, 251 (1989).

¹³D. Averin and Yu. Nazarov, *Phys. Rev. Lett.* **65**, 2446 (1990).

Translated by D. Parsons